Report 4662

DAVID W. TAYLOR
NAVAL SHIP RESEARCH AND DEVELOPMENT CENTER
Bethesda, Maryland 20084

TRANSONIC TURBULENT VISCOUS-INVISCID INTERACTION OVER AIRFOILS

by
Tsze C. Tai

Reprint from Paper 75-78 as authorized by
AIAA in letter of June 1975

AVIATION AND SURFACE EFFECTS DEPARTMENT
RESEARCH AND DEVELOPMENT REPORT

January 1976

Report 4662

TRANSONIC TURBULENT VISCOUS-INVISCID INTERACTION OVER AIRFOILS

MAJOR DTNSRDC ORGANIZATIONAL COMPONENTS

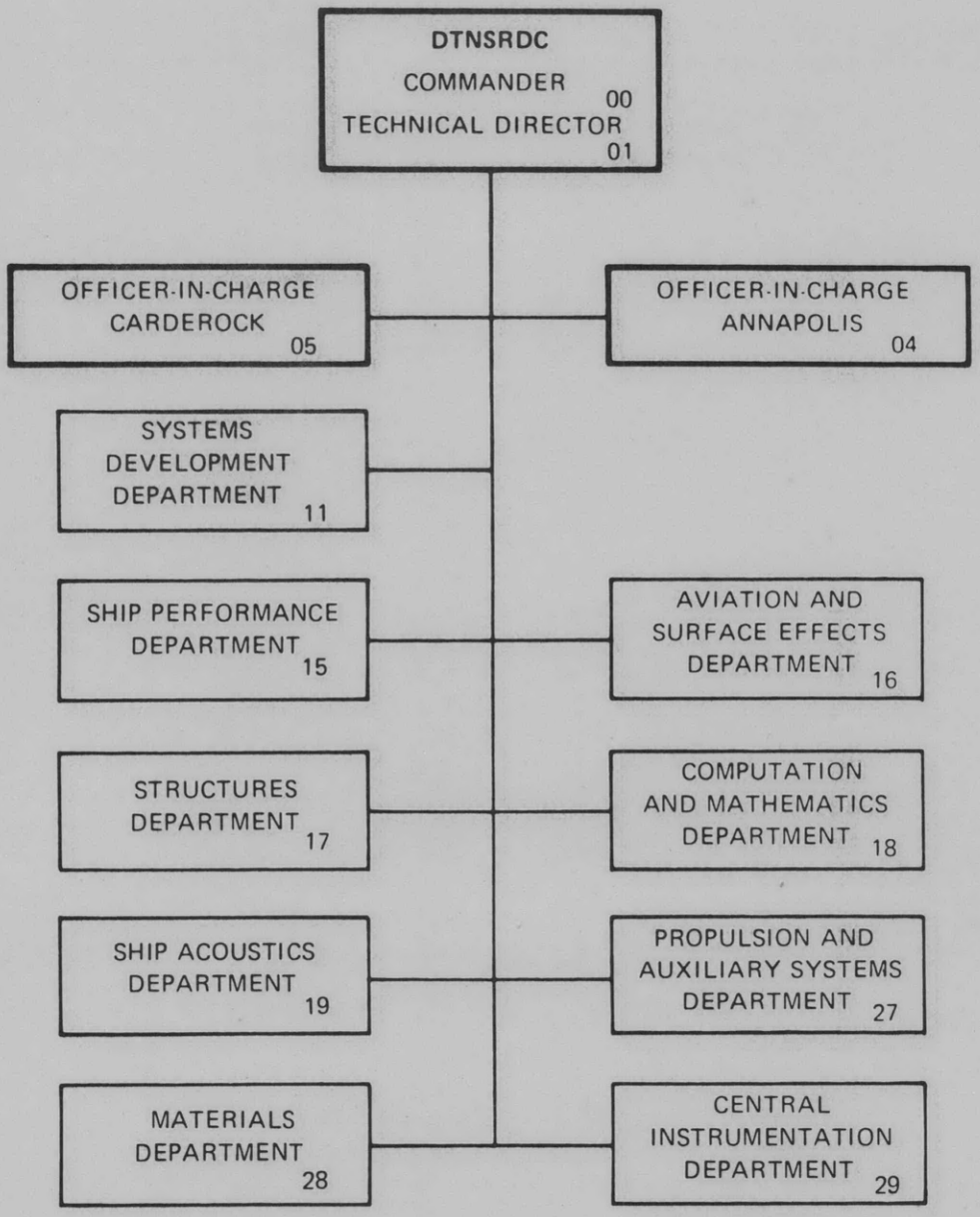

NDW-NSRDC 3960/44 (REV. 8-71)

GPO 888-302

UNCLASSIFIED

SECURITY CLASSIFICATION OF THIS PAGE (When Data Entered)

REPORT DOCUMENTATION PAGE		READ INSTRUCTIONS BEFORE COMPLETING FORM
1. REPORT NUMBER 4662	2. GOVT ACCESSION NO.	3. RECIPIENT'S CATALOG NUMBER
4. TITLE (and Subtitle) TRANSONIC TURBULENT VISCOUS-INVISCID INTERACTION OVER AIRFOILS		5. TYPE OF REPORT & PERIOD COVERED 6. PERFORMING ORG. REPORT NUMBER Aero Report 1207
7. AUTHOR(s) Tsze C. Tai		8. CONTRACT OR GRANT NUMBER(s)
9. PERFORMING ORGANIZATION NAME AND ADDRESS David W. Taylor Naval Ship R&D Center Bethesda, Maryland 20084		10. PROGRAM ELEMENT, PROJECT, TASK AREA & WORK UNIT NUMBERS Work Unit 4-1600-001
11. CONTROLLING OFFICE NAME AND ADDRESS Naval Air Systems Command (AIR-320) Washington, D.C. 20361		12. REPORT DATE January 1976 13. NUMBER OF PAGES 16
14. MONITORING AGENCY NAME & ADDRESS(if different from Controlling Office)		15. SECURITY CLASS. (of this report) UNCLASSIFIED 15a. DECLASSIFICATION/DOWNGRADING SCHEDULE

16. DISTRIBUTION STATEMENT (of this Report)

APPROVED FOR PUBLIC RELEASE: DISTRIBUTION UNLIMITED

17. DISTRIBUTION STATEMENT (of the abstract entered in Block 20, if different from Report)

18. SUPPLEMENTARY NOTES

Presented at the AIAA 13th Aerospace Sciences Meeting in Pasadena, California, on 20-22 January 1975; AIAA Paper 75-78.

19. KEY WORDS (Continue on reverse side if necessary and identify by block number)

Transonic Flow
Integral Relations
Turbulent Viscous-Inviscid Interaction
Lifting Airfoils

20. ABSTRACT (Continue on reverse side if necessary and identify by block number)

A theoretical model is formulated consisting of both inviscid external and viscous boundary-layer flows. The former is solved by the method of integral relations; the latter, by the integral method. Both attached and separated boundary layers are considered for either

(Continued on reverse side)

DD FORM 1 JAN 73 1473 EDITION OF 1 NOV 65 IS OBSOLETE
S/N 0102-014-6601

UNCLASSIFIED

SECURITY CLASSIFICATION OF THIS PAGE (When Data Entered)

(Block 20 continued)

weak or strong interactions. In case of strong interaction, the surface pressure is calculated by the viscous system rather than prescribed by the inviscid solution. The systems of resulting ordinary differential equations for both flows are coupled by the flow angle at the edge of the boundary layer. The weak interaction is accounted for by simply correcting the airfoil surface with the boundary layer-displacement thickness. The theoretical results are in fair agreement with recent turbulent experimental data.

TABLE OF CONTENTS

LIST OF FIGURES

TRANSONIC TURBULENT VISCOUS-INVISCID INTERACTION OVER AIRFOILS

Tsze C. Tai*
Naval Ship Research and Development Center
Bethesda, Maryland

Abstract

A theoretical model is formulated consisting of both inviscid external and viscous boundary-layer flows. The former is solved by the method of integral relations; the latter, by the integral method. Both attached and separated boundary layers are considered for either weak or strong interactions. In case of strong interaction, the surface pressure is calculated by the viscous system rather than prescribed by the inviscid solution. The systems of resulting ordinary differential equations for both flows are coupled by the flow angle at the edge of the boundary layer. The weak interaction is accounted for by simply correcting the airfoil surface with the boundary layer-displacement thickness. The theoretical results are in fair agreement with recent turbulent experimental data.

Nomenclature

a	Speed of sound
C	$= 1 + 2/[(\gamma-1)M_\infty^2]$
C_p	Pressure coefficient
c	Chord length of an airfoil
E_{ij}	Functions defined in Eqs. (A-1)-(A-9)
K	$= 1/(\gamma M_\infty^2)$
M	= Mach number
P	Static pressure normalized by its free-stream value
Q_j, R_j	Functions defined in Eqs. (A-10)-(A-14)
Re	Reynolds number
S	Entropy
s,n	Orthogonal curvilinear coordinates measured along and normal to the airfoil surface, normalized by the chord length
U,V	Velocity components in Cartesian coordinates, normalized by the free-stream velocity
u,v	Velocity components along and normal to the airfoil surface, normalized by the free-stream velocity
$\bar{u},\bar{v}$	Velocity components in transformed incompressible plane
u_β	Wake velocity
u_τ	Friction velocity
V_∞	Free-stream velocity
x,y	Cartesian coordinates normalized by the chord length
α	Angle of attack
β	Eddy viscosity parameter, $1 + \epsilon/\mu$
γ	Specific heat ratio
δ	Transformed boundary layer thickness
δ^*	Transformed boundary layer displacement thickness
ϵ	Eddy viscosity
η^+	$= u_\tau \eta/\nu$
Θ	Flow angle at the edge of boundary layer with respect to local surface
θ	Surface inclination with respect to the direction of free-stream velocity
μ	Fluid viscosity
ν	Kinematic viscosity
ξ,η	Coordinates in transformed incompressible plane
ρ	Gas density normalized by its free-stream value
τ_w	Shear stress at wall

Subscripts

e	Edge of boundary layer
j	jth field strip boundary
t	Total
o	Initial condition
$1,2$	Conditions before and after shock wave
∞	Free-stream condition

Introduction

In analysis of viscous transonic flows, it is needful for the analytical model of the viscous system to have the capability for allowing communication of positive pressure disturbance from the embedded shock wave upstream through the subsonic

This research was sponsored by the Naval Air Systems Command (AIR-320). The author wishes to thank Dr. H. R. Chaplin, Jr., for his interest and support and Dr. S. de los Santos for his valuable suggestions and encouragement. Thanks are also due to Drs. G. D. Kuhn, J. N. Nielsen, and I. E. Alber for helpful discussions.

*Aerospace Engineer, Aviation and Surface Effects Department. Member AIAA

portion of the boundary layer. The surface pressure should be calculated by the viscous equations rather than specified by the inviscid system. The communication of the pressure disturbance through the viscous layer becomes possible in the sense that the flow inside the viscous layer is subcritical, and the boundary layer is no longer dictated by a specified distribution of inviscid pressure. The viscous system is linked to the inviscid system through a common variable by which the change of flow properties of the outer flow may be transmitted to the inner flow or vise versa. It reflects the physical phenomenon of the shock wave/boundary-layer interaction process wherein there is a steep pressure rise before the arrival of the shock wave because of the influence exerted by the shock. This concept of the new viscous system has been explored in laminar flows by Lees and Reeves[1] and Klineberg and Lees[2] for cases with supersonic external flows and by Klineberg and Steger[3] and Tai[4] in transonic flows.

Although the laminar flow yields an adequate model for assessing the basic mechanism of the strong viscous-inviscid interaction process, flows of practical interest at transonic speeds are generally in the range of turbulent flows associated with their high Reynolds numbers. The principal difference between the laminar and turbulent viscous-inviscid interactions is that the pressure rises more rapidly for turbulent than for laminar layers,[5,6] while the displacement thickness of the boundary layer increases considerably through the shock, more so for laminar than for turbulent layers.[7] Reynolds number has a strong effect on interaction in the case of laminar boundary layers but almost no effect for turbulent flows.[5,7] The broad features of the interaction between shock wave and turbulent boundary layer over airfoils at transonic speeds have been discussed in detail by Pearcey et al.[8] Previous analyses in the area of turbulent viscous-inviscid interactions have been developed by Enseki[9] and Kuhn and Nielsen.[10] The former paper treats the interaction by using an integral method for unseparated boundary layers, combined with various simplified assumptions for external inviscid flow. The theory excludes shock-induced separation and thus restricts itself to a very limited class of weak interaction flows.[9] Separated flows, however, are considered in the latter paper. With the aid of an integral approach, the pressure is treated as a dependent variable with prescribed wall-shear distribution. The procedure has a capability for handling most interactions except in the shock wave region.[10]

In the present paper, the turbulent boundary layer method of Kuhn and Nielsen[10] is extended to strong interaction formulation by adding one more equation to the original ordinary viscous system. In the new viscous system, the surface pressure is calculated as well as other boundary-layer properties, including the wall-shear velocity. Similar to the analysis for the laminar viscous-inviscid interaction,[4] the inviscid flow field is calculated by the method of integral relations along with a newly developed N-2-strip integration scheme.[11,12]

Theoretical Model

In the present paper, the theoretical model for the problem of transonic, turbulent viscous-inviscid interaction over airfoils consists of an inviscid external flow and a viscous boundary-layer flow. The former is solved by the method of integral relations and the latter by an integral method. The two flows are coupled by the flow properties at the edge of the boundary layer.

As shown in Fig. 1, a typical transonic flow over a lifting airfoil would have supercritical flow over the upper surface and subcritical flow under the lower surface. In the forward region of the airfoil, even the flow is supercritical, the viscous-inviscid interaction is expected to be weak, and the boundary layer is attached. The usual formulation of the boundary-layer theory generally applies, i.e., the viscous effect can be accounted for by simply correcting the airfoil surface with the boundary layer-displacement thickness. The viscous system based on the integral method consists of the momentum and the moment of momentum equations, to be solved for the boundary-layer thickness and the friction velocity. It is referred to as the weak interaction formulation.

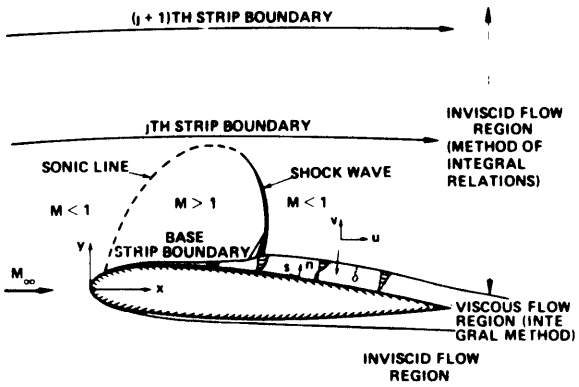

Fig. 1 - Transonic Turbulent Viscous-Inviscid Interaction Over Airfoil

For the viscous system to respond properly to the interaction of shock wave and boundary layer in which the positive pressure disturbance propagating upstream from the shock causes a steep rise in pressure, the continuity equation is coupled to the viscous system so that it becomes capable of calculating the pressure as well as other boundary layer properties. The idea is similar to that for the laminar case.[1-4] The new system is referred to as the strong interaction formulation. It is applicable to attached as well as to separated turbulent boundary layers. When applied to attached flows, the boundary layer usually separates in a short distance. If the same flow is treated by the weak interaction system, numerical experiments indicate that the boundary layer will remain attached+ until shock jump is encountered. This gives further indication that the strong interaction system is more suitable for simulating the process of shock wave/boundary-layer interaction than is the usual boundary-layer correction. However, for the region after the shock wave no matter whether the boundary layer is separat-

+Due to favorable pressure gradients generated by expansion of flow in supersonic pocket.

ed or re-attached, care must be exercised in using the strong interaction formulation to examine the downstream flow convergence. If the downstream flow does not converge to or cannot be bracketed to its proper value, the implication is that there is no need to use the strong interaction formulation in that region. The weak interaction system should be utilized instead.

For the region under the lower airfoil surface where the external inviscid flow is presumably subcritical, the weak interaction system is employed in the forward portion where the boundary layer is attached. Beyond the separation point, the viscous system is switched to the strong interaction formulation if it yields a converged flow in the downstream; otherwise, the weak interaction system remains in force in the rear zone, even the boundary layer is separated.

In summary, a strong and a weak interaction system are postulated for the viscous flow model. The former consists of continuity, the momentum, and moment of momentum equations; the latter, the momentum and the moment of momentum equations. Both formulations are valid for either attached or separated boundary layer flows.

Cartesian coordinates (x,y) are employed in the inviscid flow and surface-oriented coordinates (s,n) in the viscous flow. However, the viscous variables are computed in a transformed incompressible plane with independent variables ξ and η by means of the Stewartson transformation.

Inviscid Flow

Same as in the laminar analysis, the ordinary system for the inviscid external flow reduced from the full Euler equations by means of the N-2-strip integration scheme associated with the method of integral relations in Cartesian coordinates are as follows:[4,12]

$$\frac{dU_e}{dx} = F_e \tag{1}$$

$$\frac{dV_e}{dx} = G_e \tag{2}$$

$$\frac{dU_j}{dx} = F_j \tag{3}$$

$$\frac{dV_j}{dx} = G_j \tag{4}$$

The pressure and density are evaluated locally with the aid of equation of state.

$$\rho_e = \left(\frac{C - U_e^2 - V_e^2}{C - 1}\right)^{\frac{1}{\gamma-1}} \tag{5}$$

$$P_e = \rho_e^{\gamma} \tag{6}$$

$$\rho_j = \left[\frac{(C-1)(P_{t_2}/\rho_{t_2})_j - U_j^2 - V_j^2}{(C-1)(P_2/\rho_2^{\gamma})_j}\right]^{\frac{1}{\gamma-1}} \tag{7}$$

$$P_j = \rho_j^{\gamma} \exp(P_2/\rho_2^{\gamma})_j \tag{8}$$

where F_e, G_e, F_j, and G_j have been given elsewhere.[4] The subscript e denotes condition at the edge of the boundary layer and the index j, the condition at the jth field strip boundary; j varies from 1 to N, where N is the number of effective regions; see Fig. 1. The total number of strips is $N = \bar{N} + 1$.

Viscous Flow

Governing Equations

The governing equations for a compressible, turbulent boundary layer in coordinates parallel and normal to the surface (s,n) are as follows:

Continuity:

$$\frac{\partial(\rho u)}{\partial s} + \frac{\partial(\rho v)}{\partial n} = 0 \tag{9}$$

s-Momentum:

$$\rho u \frac{\partial u}{\partial s} + \rho v \frac{\partial u}{\partial n} = -K \frac{dP}{ds} + \frac{1}{\rho_\infty V_\infty c} \frac{\partial}{\partial n}\left(\mu\beta \frac{\partial u}{\partial n}\right) \tag{10}$$

The boundary conditions are as follows: at the surface, $u = v = 0$. At the edge of the boundary layer, $u = u_e(s)$ for weak interaction, and $u^2 + v^2 = V_e^2/\sin^2(\Theta + \theta)$ for strong interaction. It is noticed that V_e is obtained from the inviscid solution.

Stewartson Transformation

To facilitate obtaining the solutions, the above equations are transformed into incompressible forms with the aid of the Stewartson transformation[13] along with the assumptions that the viscosity varies linearly with the temperature and that the Prandtl number equals unity.

The resulting boundary layer equations in an incompressible plane are:[10]

Continuity:

$$\frac{\partial \bar{u}}{\partial \xi} + \frac{\partial \bar{v}}{\partial \eta} = 0 \tag{11}$$

ξ-Momentum

$$\bar{u} \frac{\partial \bar{u}}{\partial \xi} + \bar{v} \frac{\partial \bar{u}}{\partial \eta} = \bar{u}_e \frac{d\bar{u}_e}{d\xi} + \frac{1}{Re_\infty} \frac{\partial}{\partial \eta}\left(\beta \frac{\partial \bar{u}}{\partial \eta}\right) \tag{12}$$

Equations (11) and (12) are therefore identical with the incompressible form. The incompressible formulation of the turbulent-velocity profiles can then be used by transforming the input quantities to the incompressible plane, performing the calculation for

an equivalent incompressible boundary layer, and transforming the results back to the compressible plane.

Integral Method

Similar to Kuhn and Nielsen,[10] Eq. (12) is integrated across the boundary layer, with $\bar{v}$ eliminated by using Eq. (11).

$$\int_0^{\delta}\left[\bar{u}\frac{\partial\bar{u}}{\partial\xi} - \frac{\partial\bar{u}}{\partial\eta}\int_0^{\eta}\frac{\partial\bar{u}}{\partial\xi}\,d\zeta - \bar{u}_e\frac{d\bar{u}_e}{d\xi} - \frac{1}{Re_\infty}\frac{\partial}{\partial\eta}\left(\beta\frac{\partial\bar{u}}{\partial\eta}\right)\right] f(\eta)\,d\eta = 0 \qquad (13)$$

where

$$f(\eta) = \eta^{\sigma};\quad \sigma = 0,1 \qquad (14)$$

are the weighting functions; $\sigma = 0,1$ corresponds to the momentum and moment of momentum equations, respectively.

To determine the strong viscous-inviscid interaction in the shock wave region, the continuity equation, Eq. (11), is also integrated in the present work. In so doing, one obtains:

$$\frac{d}{d\xi}\int_0^{\delta}\bar{u}\,d\eta - \bar{u}_e\frac{d\delta}{d\xi} = -\bar{v}_e \qquad (15)$$

It increases the capability of the present viscous system for handling the strong interaction near the shock wave, where no calculations were made in Ref. 10; see Fig. 2.

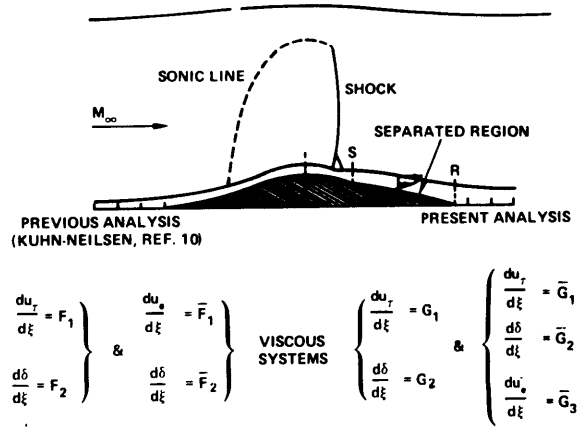

Fig. 2 - Analyses for Transonic Turbulent Viscous-Inviscid Interactions

Velocity Profile

The velocity profile utilized in performing the integration of Eqs. (13) and (15) is

$$\bar{u} = u_\tau\left[2.5\ \ell n(1+\eta^+) + 5.1 - (3.39\eta^+ + 5.1)e^{-0.37\eta^+}\right] + 0.5\,u_\beta\left[1 - \cos\left(\pi\frac{\eta}{\delta}\right)\right] \qquad (16)$$

where u_β is the wake velocity, and u_τ is the friction velocity

$$u_\tau = (\tau_w/|\tau_w|)(|\tau_w|/\rho)^{\frac{1}{2}} \qquad (17)$$

Equation (16) represents velocity profiles which are composed of an inner part, consisting of a laminar sublayer and the law-of-the-wall function, and an outer part, a wake function. It is a modification of Cole's law[14] with a laminar sublayer added.

Eddy Viscosity

The eddy viscosity model used in the present work is also similar to that of Kuhn and Nielsen,[10] except that for separated flows, the expression derived by Lees[15] is employed for the inner layer eddy viscosity. The expressions for the eddy viscosity are summarized as follows:

for attached flow, inner layer

$$\beta = 1 + 0.0533\left\{e^{0.41\bar{u}/u_\tau} - \left[1 + 0.41\frac{\bar{u}}{u_\tau} + 0.5\left(0.41\frac{\bar{u}}{u_\tau}\right)^2\right]\right\} \qquad (18)$$

for attached flow, outer layer

$$\beta = \frac{0.013 + 0.0038e^{-(\delta^*/\tau_w)(dP/d\xi)/15}}{\left[1 + 5.5\left(\frac{\eta}{\delta}\right)^6\right]}\,\bar{u}_e\delta^*Re_\infty \qquad (19)$$

for separated flow, inner layer

$$\beta = 1 + 0.018\,\bar{u}_e\eta Re_\infty\left[1 - \left(\frac{\bar{u}}{\bar{u}_e}\right)^2\right] \qquad (20)$$

for separated flow, outer layer

$$\beta = \frac{0.013\,\bar{u}_e\delta^*Re_\infty}{\left[1 + 5.5\left(\frac{\eta}{\delta}\right)^6\right]} \qquad (21)$$

Viscous Ordinary System for Strong Interactions

Substitution of Eq. (16) into Eqs. (13) and (15), with u_β eliminated by evaluating $\bar{u}$ at $\eta = \delta$, three ordinary differential equations are yielded as follows:

$$\begin{bmatrix} E_{11} & E_{12} & E_{13} \\ E_{21} & E_{22} & E_{23} \\ E_{31} & E_{23} & E_{33} \end{bmatrix} \begin{bmatrix} \frac{du_\tau}{d\xi} \\ \frac{d\delta}{d\xi} \\ \frac{d\bar{u}_e}{d\xi} \end{bmatrix} = \begin{bmatrix} Q_1 \\ Q_2 \\ Q_3 \end{bmatrix} \tag{22}$$

where E_{ij} and Q_j are presented in the appendix.

Reduced Viscous System for Weak Interactions

For the upstream region where the flow has little influence exerted by the shock wave, the viscous-inviscid interaction is weak and therefore the viscous effect can be accounted for by augmenting the airfoil surface with the boundary-layer displacement thickness in accordance with the usual formulation of the boundary-layer theory. The static pressure at the edge of the boundary layer is specified; therefore, the $d\bar{u}_e/d\xi$ becomes an input term. The viscous system consists of only the momentum and the moment of momentum equations as follows:

$$\begin{bmatrix} E_{11} & E_{12} \\ E_{21} & E_{22} \end{bmatrix} \begin{bmatrix} \frac{du_\tau}{d\xi} \\ \frac{d\delta}{d\xi} \end{bmatrix} = \begin{bmatrix} R_1 \\ R_2 \end{bmatrix} \tag{23}$$

where R_j's are listed in the appendix, and E_{ij}'s are the same as appeared in Eqs. (22)

Equations (23) are also applicable in regions where the outer inviscid flow is subcritical.

Initial Conditions

The initial values for the viscous variables are evaluated based on Schlichting's skin-friction formula for incompressible flow[16] modified for taking account of the pressure gradient.

$$u_\tau = \frac{0.122}{Re_\infty^{0.1}} \frac{\bar{u}_e^{\,1.24 + 0.24/m}}{\left[\int_0^\xi u_e^{\,3.4 + 2.4/m} d\zeta\right]^{0.1}} \tag{24}$$

and

$$\delta^* = \frac{1.4}{\bar{u}_e^{\,3.4}} \left[\frac{k(m+1)}{m Re_\infty^{1/m}} \int_0^\xi \bar{u}_e^{\,3.4+0.24/m} d\zeta\right]^{\frac{m}{m+1}} \tag{25}$$

where the quantities k and m depend to a certain extent on the Reynolds number. For the present problem, the values suggested by Eq. (21.12) of Ref. 16 were used.

$$m = 4, \quad k = 0.0128$$

For a given initial station where $\bar{u}_e$ value is known, u_τ, δ^*, and δ are found and so is the initial velocity profile.

Coupling of Two Flows

Similar to the laminar analysis,[4] the viscous system is coupled directly to the inviscid system by the induced angle of inviscid streamline at the edge of the boundary layer in case of strong interactions:

$$\Theta = \sin^{-1}\left[\frac{V_{e_{(inviscid)}}}{M_e a_{e_{(viscous)}}}\right] \tag{26}$$

where V_e is calculated by the inviscid system, while the velocity magnitude $M_e a_e$ is obtained by the viscous system. The parameter Θ is a common variable for both inviscid and viscous systems and its value is governed by the viscous-inviscid interaction process. Since the two flows are coupled by the inviscid streamline angle rather than the streamline itself, mass transfer between the outer inviscid and inner boundary layer flows is allowed in accordance with the continuity equation.

$$\frac{d\delta}{ds} = \tan\Theta + \frac{1}{\rho_e u_e} \frac{d}{ds}\left[\rho_e u_e(\delta - \delta^*)\right] \tag{27a}$$

or

$$\frac{d\delta^*}{ds} = \tan\Theta + (\delta - \delta^*) \frac{d}{ds} \ell n(\rho_e u_e) \tag{27b}$$

It is apparent that Θ has direct bearing on the growth of the boundary layer.

Since the velocity at the edge of the boundary layer is found from the viscous system, Eq. (32), its horizontal component in the compressible plane is then determined by the relation:

$$U_e = (\bar{u}_e a_\infty / a_e - V_e \sin\theta) \sec\theta \tag{28}$$

Therefore, Eq. (1) of the inviscid system, which also gives U_e, becomes redundant.

For weak interactions, the inviscid and viscous flows are linked indirectly. As in a usual procedure, the boundary layer quantities are calculated based on the specified inviscid pressure distribution and the inviscid solution is updated based on the surface augmented by the boundary layer displacement thickness. In so doing, the two flows are connected at the locus of the boundary layer displacement thickness. The latter serves as a streamline through which mass transfer, or more importantly, direct communication between the outer inviscid and inner boundary layer flows is prohibited. The inclination of the "streamline" passing through the effective surface for determining the inviscid solution is:

$$\Theta + \theta = \tan^{-1}\left(\frac{d\delta^*}{ds}\right) + \tan^{-1}\left(\frac{dy}{dx}\right) \tag{29a}$$

or

$$\Theta = \tan^{-1}\left(\frac{d\delta^*}{ds}\right) \tag{29b}$$

If Eq. (27b) is rewritten in the form

$$\Theta = \tan^{-1}\left[\frac{d\delta^*}{ds} - (\delta - \delta^*) \frac{d}{ds} \ell n(\rho_e u_e)\right] \tag{27c}$$

It is obvious that the $(\delta-\delta^*)(d/ds)\ln(\rho_e u_e)$ term has been neglected in the conventional boundary layer correction procedure. Its effect is mostly predominate in the region in front of the shock wave where the inviscid flow is locally supersonic; the flow is inclined for expansion at smaller Θ values and compression at larger Θ values. Consequently, the supersonic region has to be terminated by a sudden pressure jump at the shock wave even with the effective airfoil surface updated with boundary layer displacement thickness. The above argument is consistent with the previous statements on inadequacy of weak interaction formulation for detecting communication of the positive pressure disturbance from the shock wave.

The inviscid equations associated with the weak interaction are the same for the strong interaction except that here Eq. (9) for U_e must be used and Eq. (10) for V_e is replaced by the condition at the edge of the boundary layer.

$$V_e = U_e \tan(\Theta + \theta) \qquad (30)$$

Numerical Calculations

With the previously mentioned set of ordinary differential equations for both inviscid, Eqs. (1) to (4), and viscous flows, Eqs. (22) or (23), the numerical integrations were carried out simultaneously for both flows along the longitudinal axis x by using a standard fourth-order Runge-Kutta method. Similar to the laminar problem, the complete solution procedure consists of five iteration processes. Among which four processes, namely, those for the upstream integration, treatment of sonic point, integration for subcritical flow and enforcement of Kutta condition are exactly the same as discussed in the laminar analysis.[4] The new iteration in the present work involves adjustment of the flow angle at the edge of the boundary layer at the juncture of the weak and strong interaction regions. It replaces the iteraction procedure for determination of initial location of the strong interaction region in the laminar case.[4] The reason for the replacement is that in the turbulent case, when the flow enters the strong interaction zone, it turns away from the surface in response to a rapid separation bubble growth, triggered from the toe of the shock; see Ref. 8. The mechanism of turbulent viscous-inviscid interaction differs from that of laminar interaction. For the latter case, the compression before the shock is fairly long and smooth and involves no rapid change in the flow angle at the edge of the boundary layer; see Fig. 3.

The numerical integration first starts from the upstream and proceeds to the airfoil region. Since there is little influence exerted by the shock wave in the forward portion of the airfoil, the viscous quantities are calculated by the weak-interaction formulation, i.e., the usual boundary-layer correction. The calculated boundary layer-displacement thickness is then superimposed to the airfoil surface, and the inviscid flow is recalculated, based on the new airfoil surface. The procedure is repeated until the variation in augmented surface becomes minimal.

As the integration proceeds, the velocity at the edge of the boundary layer approaches the sonic value. The sonic point causes a singularity of the inviscid system.[12] Here the solution not only is updated for the boundary-layer correction as mentioned before but also has to satisfy the regularity condition at the sonic point. This is done by varying one of the inviscid-flow parameters, namely, the flow inclination at the strip boundary adjacent to the airfoil surface. Fig. 4 shows velocity gradients near the sonic point with viscous corrections over a 10-percent bump at $M_\infty = 0.7325$. The solid curves with various V_{1i} values are branch solutions of the subject eigenvalue problem. Each solid curve represents a viscously corrected and converged solution.

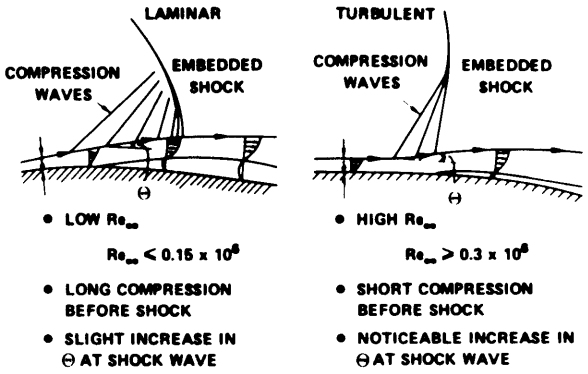

Fig. 3 - Comparison of Laminar and Turbulent Viscous-Inviscid Interactions

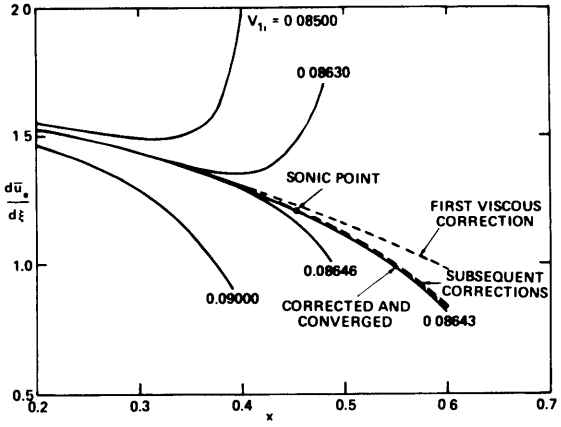

Fig. 4 - Velocity Gradients near the Sonic Point with Viscous Corrections

The boundary-layer flow so far has been attached. The positive pressure disturbance caused by the shock wave propagating upstream is almost undetected by the flow because the boundary-layer behavior is practically dictated by the prescribed inviscid-pressure distribution in the weak interaction formulation. In such a conventional formulation, the flow experiences the shock wave by a sudden pressure jump rather than a gradual pressure rise as experimentally observed.

At this stage, therefore, the integration is switched to the strong interaction formulation a

short distance in front of the shock wave. The location of the shock wave, however, is determined by the inviscid method. The boundary-layer quantities u_τ and δ are assumed to be continuous at the juncture of the two regions. The inviscid and viscous equations are integrated simultaneously with the flow angle at the edge of the boundary layer as the common variable. The value of this angle is adjusted at the juncture so that a converged flow in far downstream may be obtained by a bracketing procedure, i.e., the free-stream static pressure value is bracketed by two integral curves based on two flow angles.[12] The boundary layer is attached at the start of the strong interaction region; however, it usually separates in a short distance. Computation is then switched to the subroutines based on separated velocity profiles of the strong interaction system. Fine adjustment is made by varying the u_τ values for the convergence of the flow downstream of the separation point as shown in Fig. 5. Integration then proceeds through the shock wave region and toward the trailing edge. In the region near the trailing edge where the viscous-inviscid interaction attenuates, use of strong interaction subroutines is examined whether it leads to divergent flow downstream. Otherwise the weak interaction system is employed even for separated turbulent boundary layers.

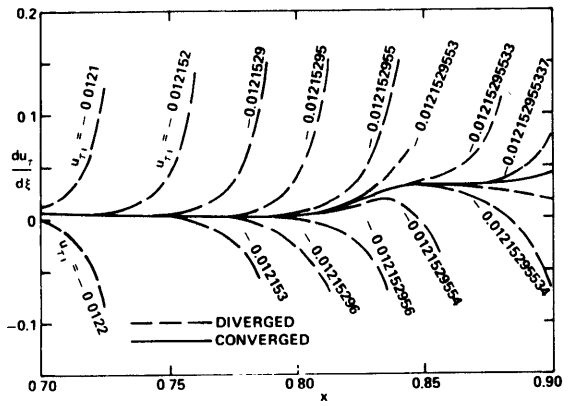

Fig. 5 - Friction Velocity Gradients Downstream of the Separation Point

The procedure for numerical integration in the lower surface follows the same pattern as for the upper surface, if the flow is supercritical. If the flow is subcritical, weak interaction usually exists for both attached and separated boundary layers. When the numerical integration along the upper and lower surface reaches the trailing edge, the resulting static pressure should be equal in order to satisfy the Kutta condition. The iteration procedures for the subcritical flow and the enforcement of the Kutta condition at the trailing edge are identical to those as in the laminar case.[4]

Results and Discussion

Results of calculations at supercritical free-stream Mach numbers are presented for a 10-percent thickness bump and an NACA 0015 airfoil at an angle of attack. Flow conditions were chosen to enable comparisons with available experimental data. The viscous results were calculated in terms of boundary layer quantities in a transformed incompressible plane and were then transformed back to a compressible plane.

10-Percent Thickness Bump

The bump is basically a 10-percent circular arc, faired with cosine curves at both ends. Fig. 6 gives the typical velocity profile at different stations over the 10-percent thickness bump at $M_\infty = 0.7325$ and $Re_\infty = 1.75 \times 10^6$. The profile at $x = 0.2$ is the initial profile, calculated by using Schlichting's skin friction formula based on power law distribution.[16] Good comparison between the calculated and available measured profiles of Alber et al.[17] at $x = 0.5$ and 0.875 indicates the adequacy of the present approach.

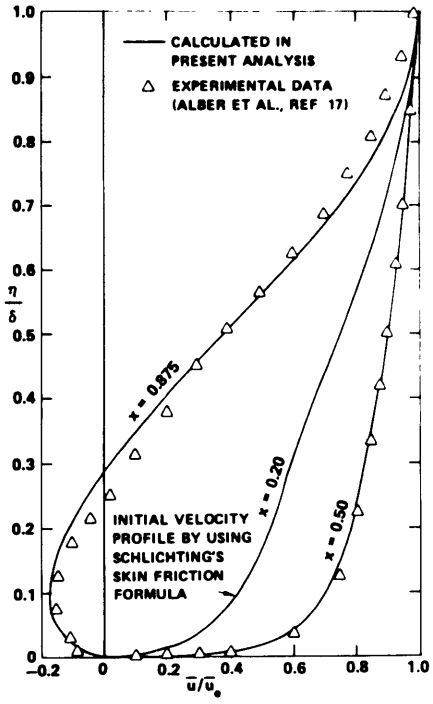

Fig. 6 - Turbulent Boundary Layer-Velocity Profiles on a 10-Percent Thickness Bump at $M_\infty = 0.7325$

Fig. 7 shows the distribution of the friction velocity over the same bump. Note that the friction velocity in the strong interaction region is calculated in the present analysis, rather than prescribed as in Ref. 10. The flow separates in a fairly short distance after it enters the strong interaction zone influenced by the shock. The friction velocity remains almost constant downstream of the separation point and then increases gradually toward reattachment.

The results for the case of a 10-percent thickness bump compare fairly well with recent turbulent experimental data of Alber et al.[17] as presented in Fig. 8. The agreement between theoretical and experimental results is good both for pressure distribution and separation point. Also plotted are the inviscid solutions obtained by using the method of integral relations with and without entropy change across the shock. Note that the shock foot is smeared as a result of the strong viscous-inviscid interaction. The compression starts at

x = 0.575 where the strong interaction begins. The turbulent boundary layer is attached throughout the supersonic region, and the strong interaction starts in front of the shock wave. Flow separation takes place downstream of the shock wave at a peak Mach number of 1.14. The trend is consistent with that found experimentally by Alber et al. (Ref. 17) for cases with $M_p < 1.32$. The turbulent boundary layer reattaches downstream of the bump. The difference between the theoretical and experimental pressures in the rear of the bump is attributed to the insufficient damping effect in the inner layer eddy viscosity model. There is also reason to believe that it may be due to overprediction of the flow by the strong interaction equations.

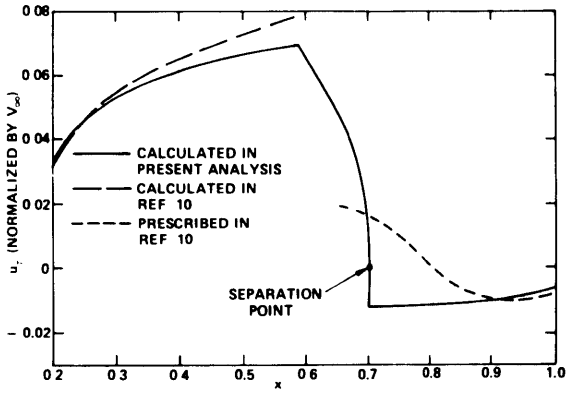

Fig. 7 - Calculated Friction-Velocity Distribution over a 10-Percent Thickness Bump at $M_\infty = 0.7325$

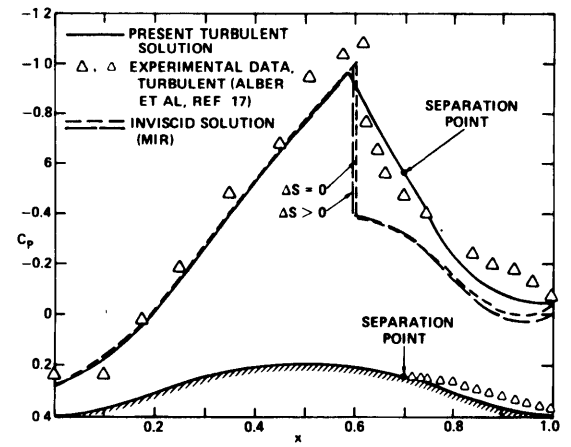

Fig. 8 - Pressure Distribution over a 10-Percent Thickness Bump at $M_\infty = 0.7325$ and $Re_\infty = 1.75 \times 10^6$

NACA 0015 Airfoil at an Angle of Attack

The flow over an NACA 0015 airfoil at $M_\infty = 0.729$ and $\alpha = 4$ deg has been investigated as an example for the lifting case. This particular flow condition has been calculated in the laminar analysis.[4] There the agreement between the laminar theory and the experiment was good except in the rear of the airfoil where the flow could have become turbulent. In the present work, therefore, the turbulent viscous-inviscid interaction model is employed for flows in the rear portion of the airfoil. The transition zone is assumed to be short enough so that the continuity of boundary layer properties may be maintained. The corresponding initial turbulent shear velocity is then estimated based on similar velocity profiles for both laminar and turbulent boundary layers. The weak interaction system is utilized in actual computation after the strong interaction formulation fails to produce a converged solution. Calculated results are given in Fig. 9 along with the previous laminar solution[4] and the experimental data of Graham et al.[18]

As indicated in Fig. 9, the pressure values over the rear region of the airfoil calculated by the present turbulent theory compare fairly well with the experimental data, Ref. 18, which were measured at Reynolds numbers on the order of 2×10^6. The flow over the upper surface has undergone strong viscous-inviscid interaction in the vicinity of the shock wave between x = 0.34 and 0.6, but it seems to have returned to weak interaction process after x = 0.6; even the boundary layer is still separated thereafter. The boundary layer remains separated all the way to the trailing edge. It follows a similar flow pattern to that observed by Pearcey et al.[8]

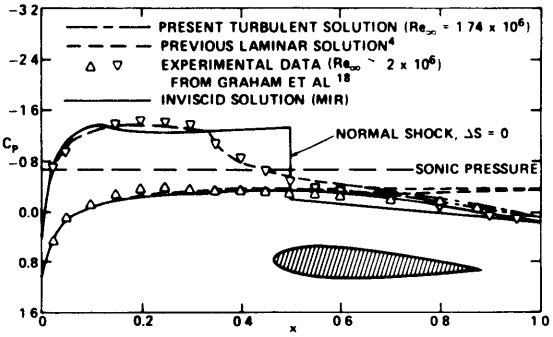

Fig. 9 - Pressure Distribution on an NACA 0015 Airfoil at $M_\infty = 0.729$ and $\alpha = 4$ Degrees

Conclusions and Recommendations

The boundary layer integral method coupled with the inviscid method of integral relations provides a relatively simple and adequate means for analyzing the essential features of transonic turbulent viscous-inviscid interaction over airfoils. The advantage of the integral relationship in both inviscid and viscous flows is that it allows the flow properties to be computed simultaneously for direct coupling of two flows in strong interaction regions. A limited comparison of the present results for surface pressure, as well as velocity profile and separation points, with available experimental data yields fairly good agreement.

In the shock wave region, the flow is characterized by the strong viscous-inviscid interaction, regardless of the boundary layer status. On the other hand, in lower subcritical flow regions, or far downstream of the shock wave, the flow may be characterized by the weak interaction, even the boundary layers are separated. It would be therefore proper to classify the level of viscous-inviscid interaction by flow regions rather than by boundary layer status.

The solution of the strong interaction formulation does not automatically approach that of the weak system when the viscous-inviscid interaction attenuates. It is therefore recommended that a rather extensive investigation be carried out to establish a rational criterion regarding the applicability of each formulation.

Unlike the laminar case, the viscous system in the strong interaction formulation has a very slow converging saddle-type singularity at zero friction. It is recommended therefore that future efforts be made to investigate the feasibility of employing a single-parameter-designated turbulent velocity profile in transonic flows so that the previously mentioned singularity may be removed.

Appendix

The E_{ij}'s and Q_j's in Eq. (33) are as follows:

$$E_{11} = \int_o^1 (2\frac{\bar{u}}{\bar{u}_e} - 1)(\frac{\partial \bar{u}}{\partial u_\tau} - a_1 \frac{\partial \bar{u}}{\partial u_\beta}) d(\frac{\eta}{\delta}) \quad \text{(A-1)}$$

$$E_{12} = \int_o^1 (2\frac{\bar{u}}{\bar{u}_e} - 1)(\frac{\partial \bar{u}}{\partial \delta} - a_2 \frac{\partial \bar{u}}{\partial u_\beta}) d(\frac{\eta}{\delta}) \quad \text{(A-2)}$$

$$E_{13} = \int_o^1 (2\frac{\bar{u}}{\bar{u}_e} - 1) \frac{\partial \bar{u}}{\partial u_\beta} d(\frac{\eta}{\delta}) - 1 \quad \text{(A-3)}$$

$$E_{21} = \int_o^1 (\frac{\partial \bar{u}}{\partial u_\beta} - a_1 \frac{\partial \bar{u}}{\partial u_\beta}) F d(\frac{\eta}{\delta}) \quad \text{(A-4)}$$

$$E_{22} = \int_o^1 (\frac{\partial \bar{u}}{\partial \delta} - a_2 \frac{\partial \bar{u}}{\partial u_\beta}) F d(\frac{\eta}{\delta}) \quad \text{(A-5)}$$

$$E_{23} = \int_o^1 \frac{\partial \bar{u}}{\partial \beta} F d(\frac{\eta}{\delta}) - 0.5 \quad \text{(A-6)}$$

$$E_{31} = \int_o^1 (\frac{\partial \bar{u}}{\partial u_\tau} - \frac{\partial \bar{u}_e}{\partial u_\tau} \frac{\partial \bar{u}}{\partial u_\beta}) d(\frac{\eta}{\delta}) \quad \text{(A-7)}$$

$$E_{32} = \int_o^1 (\frac{\partial \bar{u}}{\partial \delta} \frac{\partial \bar{u}_e}{\partial \delta} \frac{\partial \bar{u}}{\partial u_\beta}) d(\frac{\eta}{\delta}) \quad \text{(A-8)}$$

$$E_{33} = \int_o^1 \frac{\partial \bar{u}}{\partial u_\beta} d(\frac{\eta}{\delta}) \quad \text{(A-9)}$$

$$Q_1 = -\frac{\beta(\xi,0)}{Re_\infty \delta \bar{u}_e} (\frac{\partial \bar{u}}{\partial \eta})_w \quad \text{(A-10)}$$

$$Q_2 = -\frac{1}{Re_\infty \delta \bar{u}_e} \int_o^1 \beta \frac{\partial \bar{u}}{\partial \eta} d(\frac{\eta}{\delta}) \quad \text{(A-11)}$$

$$Q_3 = -V_e \quad \text{(A-12)}$$

where

$$F = 2\frac{\eta}{\delta}\frac{\bar{u}}{\bar{u}_e} - 1 - \int_o^\eta \frac{\bar{u}}{\bar{u}_e} d(\frac{\zeta}{\delta}) + \int_o^\delta \frac{\bar{u}}{\bar{u}_e} d(\frac{\eta}{\delta})$$

$$a_1 = 2.5\, ln(1+\delta^+) - (4.887 - 1.438\delta^+) e^{-0.37\delta^+} + 5.1(1-e^{-0.37\delta^+}) + \frac{2.5\delta^+}{1+\delta^+}$$

$$a_2 = u_\tau |u_\tau| Re_\infty \left[\frac{2.5}{1+\delta^+} - (1.5 - 1.25\delta^+) e^{-0.37\delta^+}\right]$$

The right-hand side of the equations for E_{ij}'s and Q_2 may be integrated numerically by using the Simpson rule.[19]

$$R_1 = -E_{13}\frac{d\bar{u}_e}{d\xi} + Q_1 \quad \text{(A-13)}$$

$$R_2 = -E_{23}\frac{d\bar{u}_e}{d\xi} + Q_2 \quad \text{(A-14)}$$

References

1. Lees, L. and Reeves, B. L., "Supersonic Separated and Reattached Laminar Flows: I. General Theory and Application of Adiabatic Boundary Layer Shock Wave Interactions," AIAA J., Vol. 2., No. 11, Nov. 1964, pp. 1907-1920.

2. Klineberg, J. M. and Lees, L., "Theory of Laminar Viscous-Inviscid Interactions in Supersonic Flow," AIAA J., Vol. 17, No. 12, Dec. 1969, pp. 2211-2221.

3. Klineberg, J. M. and Steger, J. L., "Calculation of Separated Flows at Subsonic and Transonic Speeds," Paper presented at Third International Conference on Numerical Methods in Fluid Dynamics, Paris, France, Jul. 1972.

4. Tai, T. C., "Transonic Laminar Viscous-Inviscid Interaction over Airfoils," NSRDC Rept. 4362, Jun. 1974, Naval Ship R and D Center, Bethesda, Md.; Brief version presented as AIAA Paper 74-600, Palo Alto, Calif., Jun. 1974.

5. Holder, D. W., "The Transonic Flow Past Two-Dimensional Aerofoils," J. Roy. Aeron. Soc., Vol. 68, No. 644, Aug. 1964, pp. 501-516.

6. Holder, D. W., Pearcey, H. H. and Gadd, G. E., "The Interaction between Shock Waves and Boundary Layers," Aeron. Res. Council CP 180, 1954, London, England.

7. Ackeret, J., Feldmann, F., and Rott, N., "Investigation of Compression Shocks and Boundary Layers in Gases Moving at High Speeds," 1947, TM 1113, NACA.

8. Pearcey, H. H., Osborne, J. and Haines, A. B., "The Interaction between Local Effects at the Shock and Rear Separation — a Source of Significant Scale Effects in Wind-Tunnel Tests on Aerofoils and Wings," in "Transonic Aerodynamics," CP 35, Sep. 1968, AGARD.

9. Enseki, F. K., "A Calculative Method for the Turbulent Transonic Viscous-Inviscid Interaction on Airfoils," presented as AIAA Paper 72-5, San Diego, Calif., Jan. 1972.

10. Kuhn, G. D. and Nielsen, J. N., "Prediction of Turbulent Separated Boundary Layers," presented as AIAA Paper 73-663, Palm Springs, Calif., Jul. 1973.

11. Tai, T. C., "Application of the Method of Integral Relations to Transonic Airfoil Problems: Part I — Inviscid Supercritical Flow over Symmetric Airfoil at Zero Angle of Attack," NSRDC Rept. 3424, Sep. 1970; "Part II — Inviscid Supercritical Flow about Lifting Airfoils with Embedded Shock Wave," NSRDC Rept. 3424-II, Jul. 1972, Naval Ship R and D Center, Bethesda, Md.

12. Tai, T. C., "Transonic Inviscid Flow over Lifting Airfoils by the Method of Integral Relations," AIAA J., Vol. 12, No. 6, Jun. 1974, pp. 798-804.

13. Stewartson, K., "Correlated Incompressible and Compressible Boundary Layers," Proc. Roy. Soc., Ser. A, Vol. 200, 1949, London, England, pp. 85-100.

14. Coles, D., "The Law of the Wake in the Turbulent Boundary Layer," J. of Fluid Mech., Vol. 1, Pt. 2, Jul. 1956, pp. 191-226.

15. Lees, L., "Turbulent Boundary Layer with Vanishing or Small Skin Friction," SAMSO TR 70-97, 1970, TRW Systems Group, Redondo Beach, Calif.

16. Schlichting, H, "Boundary Layer Theory," 6th English Edition, McGraw-Hill, New York, 1968, p. 600.

17. Alber, I. E., Bacon, J. W., Masson, B. S., and Collins, D. J., "An Experimental Investigation of Turbulent Transonic Viscous-Inviscid Interactions," AIAA Jour., Vol. 11, No. 5, May 1973, pp. 620-627.

18. Graham, D. J., Nitzberg, G. E. and Olson, R. N., "A Systematic Investigation of Pressure Distribution at High Speeds over Five Representative NACA Low-Drag and Conventional Aerofoil Sections," Rept. 832, 1945, NACA.

19. Southworth, R. W. and Deleeuw, S. L., "Digital Computation and Numerical Methods," McGraw-Hill, New York, 1965, pp. 371-375.

INITIAL DISTRIBUTION

Copies		Copies	
1	Chief of R&D (ABMDA)	1	National Sci Foundation
1	U.S. Army Missile Command	1	Argonne National Lab T.C. Chawla
3	CHONR 1 430B 1 432 1 461	1	U of Akron/Lib
		1	Brown U/Div of Engr
1	NRL	1	Calif Inst of Tech Grad Aero Labs
4	ONR 1 Boston 1 Chicago 1 London, England 1 Pasadena	1	Calif Inst of Tech/Jet Prop Lab D.J. Collins
		2	U of Calif 1 Dr. M. Holt/Div Aero Sciences 1 Lib
1	USNA		
1	USNPGSCOL		
1	NAVAIRDEVCEN	2	U of Calif 1 Dr. J.D. Coles/Engr & Appl Sciences 1 Lib
1	NWC		
1	NSWC/White Oak		
1	NSWC/Dahlgren	1	U of Calif at LaJolla/Lib
13	NAVAIRSYSCOM 1 AIR 03A 1 AIR 03C 1 AIR 310 3 AIR 320 1 AIR 5108 4 AIR 5301 2 AIR 604	1	U of S Calif/Lib
		1	Catholic U of America/Lib
		1	U of Cincinnati/ Aerospace Engr
		2	Clemson U 1 Dr. T. Yang/Mech Engr Dept 1 Lib
1	NAVSEASYSCOM		
12	DDC	1	Cornell U/Lib
1	AFOSR	1	Georgia Inst Tech/Lib
1	USAFA	1	Harvard U/Gordon McKay Lib
1	AF INST TECH		
1	AEDC	1	Johns Hopkins U/Lib
4	NASA 1 HQ, Washington, D.C. 1 Ames Research Cen/Lib 1 Langley Research Center 1 Lewis Research Center	1	U of Illinois/Lib
		1	U of Maryland/Lib
		1	MIT/Lib
		2	U of Michigan 1 Aerospace Engr 1 Lib

Copies	
2	New York U/Courant Inst Math Sci 1 Dr. P.R. Garabedian 1 Dr. D.G. Korn
1	U of N Carolina/Lib
2	N Carolina State U/Raleigh 1 Dr. F.R. DeJarnette/Mech & Aerospace Engr Dept 1 Lib
1	Pennsylvania State U/Lib
1	Princeton U/Lib
1	Purdue U/Lib
1	Stanford U/Lib
2	U of Tennessee Space In 1 Dr. J.M. Wu 1 Lib
1	U of Virginia/Alderman Lib
2	Virginia Polytech Inst 1 Carol M. Newman Lib 1 Aerospace Engr Dept
1	U of Washington/Lib
1	W Virginia U/Dept Aero Engr
1	American Inst of Aeronautics & Astronautics
1	ARO Inc/Lib
1	Boeing Company/Seattle
1	Calspan Corp./Buffalo
1	Flow Corp, Inc./Dr. E.M. Murman
1	General Dynamics Convair/Lib
1	Grumman Aerospace Corp/Lib
1	Inst for Defense Analyses
1	Lockheed-Georgia Co/Lib
1	Lockheed Missiles & Space Co/Lib

Copies	
1	LTV Aerospace Corp/Lib
1	McDonnell Douglas St. Louis/Lib
1	Douglas Aircraft Co/Lib
1	Nielsen Engr & Res Inc
1	Rockwell International Corp/Lib
1	Northrop Corporate Labs/ Lib
1	TRW Systems Group/Lib

CENTER DISTRIBUTION

Copies	Code	
1	1541	P.S. Granville
10	1600	H.R. Chaplin
1	1606	S. de los Santos
25	1606	T.C. Tai
1	1840	H. Lugt
30	5211	Reports Distribution
1	5221	Library (C)
1	5222	Library (A)
2	5223	Aerodynamics Lib